

# A Possible Detection of the Cosmic Antineutrino Background in the Presence of Flavor Effects

Y.F. Li <sup>1</sup> and Zhi-zhong Xing <sup>2</sup>

Institute of High Energy Physics & Theoretical Physics Center for Science Facilities,  
Chinese Academy of Sciences, Beijing 100049, China

## Abstract

Lusignoli and Vignati have recently pointed out that it is in principle possible to directly detect the cosmic *antineutrino* background (C $\bar{\nu}$ B) by using the rather stable isotope  $^{163}\text{Ho}$  as a target, which can decay into  $^{163}\text{Dy}$  via electron capture (EC) with a very small energy release. In this paper we calculate the rate of the relic antineutrino capture on  $^{163}\text{Ho}$  nuclei against the corresponding EC decay rate by taking account of different neutrino mass hierarchies and reasonable values of  $\theta_{13}$ . We show that such flavor effects are appreciable and even important in some cases, and stress that a calorimetric C $\bar{\nu}$ B measurement might be feasible in the future.

*Keywords:* neutrino mass hierarchy; isotope  $^{163}\text{Ho}$ ; cosmic antineutrino background

---

<sup>1</sup>E-mail: liyufeng@ihep.ac.cn

<sup>2</sup>E-mail: xingzz@ihep.ac.cn

The standard cosmology predicts that relic neutrinos and antineutrinos of the Big Bang must survive today and form a cosmic background, but their average temperature is so low ( $T_\nu \simeq 1.945$  K) that their existence has not directly been verified [1]. Among several proposals for a direct detection of the cosmic *neutrino* background (C $\nu$ B) [2], the most promising one should be the neutrino capture experiment by means of radioactive  $\beta$ -decaying nuclei [3]–[11]. A direct measurement of the cosmic *antineutrino* background (C $\bar{\nu}$ B) could similarly be done by using radioactive nuclei which can decay via electron capture (EC) [12], but it seems much less hopeful.

Lusignoli and Vignati have recently pointed out an interesting and noteworthy way to directly detect the C $\bar{\nu}$ B [13]. It takes advantage of the rather stable isotope  $^{163}\text{Ho}$  as a target, which undergoes an EC decay into  $^{163}\text{Dy}$  with a small energy release ( $Q \simeq 2.5$  keV). The signature of this relic antineutrino capture process is located on the right-hand side of the spectral endpoint of the EC decay, and their interval is detectable if the experiment has a sufficiently good energy resolution. In practice, it is promising to do a high-statistics *calorimetric* experiment to measure the  $^{163}\text{Ho}$  spectrum, probe the absolute neutrino mass scale [14] and even detect the C $\bar{\nu}$ B.

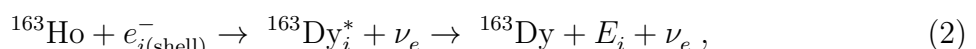
In this paper we shall calculate the rate of the relic antineutrino capture on  $^{163}\text{Ho}$  nuclei against the corresponding EC decay rate by taking account of different neutrino mass hierarchies and reasonable values of the smallest neutrino mixing angle  $\theta_{13}$ . Such flavor effects, which were not considered in Ref. [13], are found to be appreciable and even important in some cases. We shall first look at the energy spectrum of the EC decay of  $^{163}\text{Ho}$  by examining how sensitive the ratios of the peak heights and the fine structure near the spectral endpoint are to the neutrino mass hierarchy, and then present a detailed analysis of flavor effects on the detection of the C $\bar{\nu}$ B by using a target made of this isotope. Although our numerical results are mainly for the purpose of illustration, we stress that such a direct laboratory measurement of the C $\bar{\nu}$ B deserves further attention and investigations and might be feasible in the long term.

The key point of the relic antineutrino capture on  $^{163}\text{Ho}$  nuclei is to capture the relic *electron* antineutrinos in a way without any energy threshold. In the three-flavor scheme the  $|\nu_e\rangle$  and  $|\bar{\nu}_e\rangle$  states are superpositions of three neutrino and antineutrino mass eigenstates, respectively:

$$\begin{aligned} |\nu_e\rangle &= \sum_k V_{ek}^* |\nu_k\rangle , \\ |\bar{\nu}_e\rangle &= \sum_k V_{ek} |\bar{\nu}_k\rangle , \end{aligned} \quad (1)$$

where  $V_{ek}$  (for  $k = 1, 2, 3$ ) denotes an element in the first row of the  $3 \times 3$  neutrino mixing matrix  $V$ . We have  $|V_{e1}| = \cos \theta_{12} \cos \theta_{13}$ ,  $|V_{e2}| = \sin \theta_{12} \cos \theta_{13}$  and  $|V_{e3}| = \sin \theta_{13}$  in the standard parametrization of  $V$  [15], where  $\theta_{12} \simeq 34^\circ$  and  $\theta_{13} < 12^\circ$  as indicated by a global analysis of current neutrino oscillation data [16]. Of course,  $\theta_{13} = 0^\circ$  and  $\theta_{13} \neq 0^\circ$  may have very different consequences in neutrino phenomenology, as we shall see later on.

Now let us consider the EC decay of the isotope  $^{163}\text{Ho}$  [17]:



where  $e_{i(\text{shell})}^-$  denotes an orbital electron from the  $i$ -th shell of holmium-163, and  $E_i$  is the corresponding binding energy of the electron hole in dysprosium-163. If the  $Q$ -value

of this EC decay is defined as the mass difference between the two atoms in their ground states, then the energy spectrum of the outgoing neutrinos will be given by a series of lines at  $Q - E_i$ . Note that  $Q$  has not well been determined and its value is possible to range from 2.3 keV to 2.8 keV [13]. In what follows we shall take  $Q = 2.5$  keV as a default value unless otherwise explicitly mentioned. Taking account of the Breit-Wigner resonance form of the atomic levels [17], one may express the energy spectrum of the detected EC events as follows:

$$\frac{d\lambda_{\text{EC}}}{dT_c} = \frac{G_\beta^2}{4\pi^2} (Q - T_c) \sum_k |V_{ek}|^2 \sqrt{(Q - T_c)^2 - m_k^2} \Theta(Q - T_c - m_k) \times \sum_i n_i C_i \beta_i^2 B_i \frac{\Gamma_i}{2\pi} \cdot \frac{1}{(T_c - E_i)^2 + \Gamma_i^2/4}, \quad (3)$$

where  $\lambda_{\text{EC}}$  denotes the rate of this EC decay,  $T_c$  is the so-called “calorimetric” energy which measures the difference between  $Q$  and the neutrino energy [18],  $G_\beta \equiv G_F \cos \theta_C$  with  $\theta_C \simeq 13^\circ$  being the Cabibbo angle of quark flavor mixing,  $m_k$  is the mass of  $\bar{\nu}_k$  (for  $k = 1, 2, 3$ ), and the theta function  $\Theta(Q - T_c - m_k)$  has been imposed on Eq. (3) to ensure the kinematic requirement. In addition,  $n_i$  denotes the fraction of occupancy of the  $i$ -th electron shell,  $C_i$  is the nuclear shape factor,  $\beta_i$  represents the Coulomb amplitude of the electron radial wave function, and  $B_i$  is an atomic correction for the electron exchange and overlap. The  $Q$ -value of this EC decay is so small that only those electrons from  $M_1$ ,  $M_2$ ,  $N_1$ ,  $N_2$ ,  $O_1$ ,  $O_2$  and  $P_1$  levels can be captured [13]. In an excellent narrow-width approximation [18] the integral of Eq. (3) yields

$$\lambda_{\text{EC}} = \frac{G_\beta^2}{4\pi^2} \sum_i \sum_k n_i C_i \beta_i^2 B_i (Q - E_i) |V_{ek}|^2 \sqrt{(Q - E_i)^2 - m_k^2}, \quad (4)$$

where  $i$  runs over all the possible electron shells of  $^{163}\text{Ho}$  that involve its EC decay, and  $k$  runs over three neutrino mass eigenstates.

Given a positive  $Q$ -value, a thresholdless capture of the incoming relic antineutrinos on the EC-decaying  $^{163}\text{Ho}$  nuclei may happen through

$$\bar{\nu}_e + {}^{163}\text{Ho} + e_{i(\text{shell})}^- \rightarrow {}^{163}\text{Dy}_i^* \rightarrow {}^{163}\text{Dy} + E_i. \quad (5)$$

The capture rate for each mass eigenstate  $\bar{\nu}_k$  (for  $k = 1, 2, 3$ ) hidden in the flavor eigenstate  $\bar{\nu}_e$  can be given by

$$\lambda_{\bar{\nu}_k} = \frac{G_\beta^2}{2} n_{\bar{\nu}_k} |V_{ek}|^2 \sum_i n_i C_i \beta_i^2 B_i \frac{\Gamma_i}{2\pi} \cdot \frac{1}{(E_{\bar{\nu}_k} + Q - E_i)^2 + \Gamma_i^2/4}, \quad (6)$$

where  $n_{\bar{\nu}_k}$  and  $E_{\bar{\nu}_k}$  are the number density and energy of  $\bar{\nu}_k$ , respectively. The standard Big Bang cosmology predicts  $n_{\nu_k} = n_{\bar{\nu}_k} \simeq 56 \text{ cm}^{-3}$  today for each species of relic neutrinos and antineutrinos [1], but possible gravitational clustering of massive  $\nu_k$  and  $\bar{\nu}_k$  around the Earth could make their number densities much bigger [19]. For simplicity, we shall not consider the gravitational clustering effect in the subsequent analysis. Note that the de-excitation energy of unstable  ${}^{163}\text{Dy}_i^*$  in Eq. (5) is in principle monoenergetic for each mass eigenstate  $\bar{\nu}_k$  (i.e.,  $T_k \equiv E_{\bar{\nu}_k} + Q$ ). Convolved with a finite energy resolution in

practice, the ideally discrete energy lines of the final states in Eq. (5) must spread and then form a continuous spectrum. As usual, we consider a Gaussian energy resolution function defined by

$$R(T, T_k) = \frac{1}{\sqrt{2\pi}\sigma} \exp \left[ -\frac{(T - T_k)^2}{2\sigma^2} \right], \quad (7)$$

where  $T$  is the overall energy of an event detected in the experiment. Using  $\Delta$  to denote the experimental energy resolution (i.e., the full width at half maximum of a Gaussian energy resolution for the detected events), we have  $\Delta = 2\sqrt{2\ln 2}\sigma \approx 2.35482\sigma$ . Then the overall antineutrino capture rate reads

$$\lambda_{\bar{\nu}} = \frac{G_{\beta}^2}{2} \sum_i \sum_k n_{\bar{\nu}_k} |V_{ek}|^2 R(T, T_k) n_i C_i \beta_i^2 B_i \frac{\Gamma_i}{2\pi} \cdot \frac{1}{(T_k - E_i)^2 + \Gamma_i^2/4}. \quad (8)$$

In the mean time, the energy spectrum of the EC decay should also be convoluted with the Gaussian energy resolution. So we rewrite Eq. (3) as

$$\begin{aligned} \frac{d\lambda_{\text{EC}}}{dT} = & \int_0^{Q-\min(m_k)} dT_c \left[ \frac{G_{\beta}^2}{4\pi^2} R(T, T_c) (Q - T_c) \right. \\ & \times \sum_k |V_{ek}|^2 \sqrt{(Q - T_c)^2 - m_k^2} \Theta(Q - T_c - m_k) \\ & \times \left. \sum_i n_i C_i \beta_i^2 B_i \frac{\Gamma_i}{2\pi} \cdot \frac{1}{(T_c - E_i)^2 + \Gamma_i^2/4} \right]. \end{aligned} \quad (9)$$

The above two equations allow us to calculate the rate of the relic antineutrino capture on the EC-decaying  $^{163}\text{Ho}$  nuclei against the corresponding background (i.e., the EC decay itself) in the presence of flavor effects, which are characterized by both the neutrino masses  $m_k$  and the neutrino mixing matrix elements  $|V_{ek}|$  (for  $k = 1, 2, 3$ ).

We proceed to evaluate the flavor effects on both the relic antineutrino capture rate and the corresponding EC decay rate with the help of Eqs. (8) and (9). In our numerical calculations we take  $\Delta m_{21}^2 \approx 7.6 \times 10^{-5} \text{ eV}^2$  and  $|\Delta m_{31}^2| \approx 2.4 \times 10^{-3} \text{ eV}^2$  together with  $\theta_{12} \approx 34^\circ$  as typical inputs [16]. The impact of  $\theta_{13}$  on  $\lambda_{\bar{\nu}}$  and  $\lambda_{\text{EC}}$  can be examined by allowing its value to vary within  $0^\circ \leq \theta_{13} < 12^\circ$  [16]. Depending on the sign of  $\Delta m_{31}^2$ , two mass patterns of three active neutrinos are possible: one is the normal mass ordering with  $m_1 < m_2 = \sqrt{m_1^2 + \Delta m_{21}^2} < m_3 = \sqrt{m_1^2 + |\Delta m_{31}^2|}$ ; and the other is the inverted mass ordering with  $m_3 < m_1 = \sqrt{m_3^2 + |\Delta m_{31}^2|} < m_2 = \sqrt{m_3^2 + |\Delta m_{31}^2| + \Delta m_{21}^2}$ . In either case the absolute neutrino mass scale ( $m_1$  or  $m_3$ ) is unknown, but its upper bound is expected to be of  $\mathcal{O}(0.1) \text{ eV}$  up to  $\mathcal{O}(1) \text{ eV}$  as constrained by current experimental and cosmological data [15, 20]. As for the values of those parameters relevant to the atomic levels of  $^{163}\text{Dy}$ , we refer the reader to Ref. [13] and references therein. The energy levels of the captured electrons are assumed to be fully occupied (i.e.,  $n_i = 1$ ) and their binding energies and widths can be found in Table 1 of Ref. [13]. The atomic corrections for the electron exchange and overlap are neglected (i.e.,  $B_i \simeq 1$ ), and the ratios of the squared wave functions at the origin (i.e.,  $\beta_i^2/\beta_{M_1}^2$ ) can be found in Table 2 of Ref. [13]. Because the nuclear shape factors  $C_i$  are approximately identical in an allowed transition [17], they can be factored out from the sum in Eqs. (3), (4), (6), (8) and (9). Finally, one should

note that the numerical results of  $\lambda_{\bar{\nu}}$  and  $\lambda_{\text{EC}}$  can be properly normalized by means of the half-life of  $^{163}\text{Ho}$  through the relation  $\lambda_{\text{EC}} T_{1/2} = \ln 2$ , where  $T_{1/2} \simeq 4570$  yr. Then the distributions of the number of capture events and the number of background events are expressed, respectively, as

$$\begin{aligned} N_{\text{S}}(T) &= \frac{\lambda_{\bar{\nu}}}{\lambda_{\text{EC}}} \cdot \frac{\ln 2}{T_{1/2}} N_{\text{T}} t, \\ N_{\text{B}}(T) &= \frac{1}{\lambda_{\text{EC}}} \cdot \frac{d\lambda_{\text{EC}}}{dT} \cdot \frac{\ln 2}{T_{1/2}} N_{\text{T}} t \end{aligned} \quad (10)$$

for a given target factor  $N_{\text{T}}$  (i.e., the number of  $^{163}\text{Ho}$  atoms of the target) and for a given exposure time  $t$  in the experiment.

Let us first look at the energy spectrum of the EC decay of  $^{163}\text{Ho}$ . Our main concern is the flavor effects on the ratios of the peak heights and the fine structure near the endpoint of the energy spectrum. The numerical results are shown in Fig. 1, where  $\theta_{13} = 10^\circ$  has typically been input. Fig. 1(a) and Fig. 1(b) show that two ratios of the peak heights are completely insensitive to the lightest neutrino mass  $m_0$ , which is identified with  $m_1$  for the normal mass hierarchy (i.e.,  $m_1 < m_2 < m_3$ ) or with  $m_3$  for the inverted mass hierarchy (i.e.,  $m_3 < m_1 < m_2$ ). Given  $m_0 \leq 0.5$  eV, the actual variations of two ratios are only at the  $\mathcal{O}(10^{-6})$  level. Hence it is hopeless to obtain any information about the absolute mass scale of three neutrinos or their mass hierarchy by measuring these ratios. However, it seems very promising to acquire knowledge of the  $Q$ -value from these ratios, as one can clearly see in Fig. 1(c) and Fig. 1(d). In Fig. 1(e) and Fig. 1(f) we illustrate how the ratios of the peak heights change with the energy resolution  $\Delta$  for given values of  $m_0$  and  $Q$ . We see that the changes are at the percent level if  $\Delta \leq 1$  eV is taken.

The fine structure near the spectral endpoint of the EC decay of  $^{163}\text{Ho}$  is illustrated in Fig. 2, where  $\theta_{13} = 10^\circ$  has also been input. The location of the endpoint is essentially determined by the smallest neutrino mass. It might be possible to distinguish between the normal and inverted neutrino mass hierarchies, since they have different effects on the energy spectrum near its endpoint. Especially for the inverted mass hierarchy, an obvious distortion occurs at the position  $T_c \simeq Q - m_1$  with  $m_1 = \sqrt{m_3^2 + |\Delta m_{31}^2|}$  due to the fact that the lightest mass eigenstate  $\nu_3$  hidden in  $\nu_e$  is associated with the smallest neutrino mixing matrix element  $|V_{e3}|^2 = \sin^2 \theta_{13}$ . In the region of  $T_c > Q - m_1$ , only the  $\nu_3$  component contributes to the spectrum. In comparison, the contributions of  $\nu_1$  and  $\nu_2$  components to the spectrum are dominant in the region of  $T_c < Q - m_1$ . One might therefore be able to determine the magnitude of  $|V_{e3}|^2$  if the endpoint distortion in the energy spectrum could really be observed. A similar distortion cannot appear in the case of the normal neutrino mass hierarchy, simply because the contribution of the lightest mass eigenstate  $\nu_1$  to the spectrum is of the same order of magnitude as those of  $\nu_2$  and  $\nu_3$ .

Let us now focus on the relic antineutrino capture on  $^{163}\text{Ho}$  nuclei against the EC decay background by taking account of the flavor effects and examining the  $Q$ -value dependence. In our calculations we assume 30 kg  $^{163}\text{Ho}$  as a reference isotope source. The numerical results are presented in Fig. 3, Fig. 4 and Fig. 5, where the relic antineutrino capture rate is illustrated as a function of the overall energy release  $T$  in a possible experiment. Some comments and discussions are in order.

(1) Given  $\theta_{13} = 10^\circ$  as a typical input, Fig. 3 shows the effects of the neutrino mass hierarchy on the  $C\bar{\nu}B$  signature and the corresponding background. The value of the finite energy resolution  $\Delta$  is chosen in such a way that only a single peak of the signature can be seen; namely, at least one peak of the signature is not allowed to fall into the shade of the background. Eq. (8) tells us that the contribution of each antineutrino mass eigenstate  $\bar{\nu}_k$  (for  $k = 1, 2, 3$ ) to the capture rate is located at  $T = T_k \equiv E_{\bar{\nu}_k} + Q$  and weighted by the relic antineutrino number density  $n_{\bar{\nu}_k} \simeq 56 \text{ cm}^{-3}$  and the flavor mixing matrix element  $|V_{ek}|^2$ . On the other hand, Eq. (9) tells us that the energy spectrum of the EC decay near its endpoint is dominated by the lightest neutrino mass eigenstate hidden in  $\bar{\nu}_e$  and sensitive to the energy resolution  $\Delta$ . As the smallest neutrino mass ( $m_1$  in the left panel of Fig. 3 or  $m_3$  in the right panel of Fig. 3) increases from 0 to 0.1 eV, the  $C\bar{\nu}B$  signature moves towards the larger  $T - Q$  region. In comparison, the shift of the corresponding background is less obvious because the smallest neutrino mass and  $\Delta$  have the opposite effects on the location of the spectral endpoint of the EC decay. Hence the distance between the peak of the signature and the background becomes larger for a larger value of the smallest neutrino mass, and accordingly the required energy resolution  $\Delta$  becomes less stringent. Comparing between Fig. 3(c) and Fig. 3(d), for example, one can also see that it is more or less easier to detect the  $C\bar{\nu}B$  in the  $\Delta m_{31}^2 < 0$  case, where the signature is separated more obviously from the background. The reason is simply that the dominant antineutrino mass eigenstates  $\bar{\nu}_1$  and  $\bar{\nu}_2$  have slightly larger eigenvalues in this case than in the  $\Delta m_{31}^2 > 0$  case. Note that more than one peak may emerge in the distribution of the relic antineutrino capture rate, as shown in Fig. 3(a) and Fig. 3(b), provided the energy resolution is sufficiently good. But the requirement  $\Delta \leq m_k/2$  [6] is in general needed so as to resolve the corresponding peak.

(2) The effect of the unknown neutrino mixing angle  $\theta_{13}$  on the  $C\bar{\nu}B$  detection is examined in Fig. 4, where both the  $\Delta m_{31}^2 > 0$  case with  $m_1 = 0$  and the  $\Delta m_{31}^2 < 0$  case with  $m_3 = 0$  are taken into account. The energy resolution  $\Delta$  is chosen in such a way that the signature in Fig. 4(b) with  $m_3 = 0$  and  $\theta_{13} = 0^\circ$  should be clearly seen. In the  $\Delta m_{31}^2 > 0$  case, Fig. 4(a), Fig. 4(c) and Fig. 4(e) show that a change of  $\theta_{13}$  in its allowed region (i.e.,  $\theta_{13} < 12^\circ$ ) almost has no effect on both the signature and the background. In the  $\Delta m_{31}^2 < 0$  case, however, the background turns out to be sensitive to a change of  $\theta_{13}$  as one can see from Fig. 4(b), Fig. 4(d) and Fig. 4(f). As  $\theta_{13}$  becomes larger, the signature essentially keeps intact but the background apparently moves towards the larger  $T - Q$  region, making the signature partly fall into the shade. Note that the distribution of the  $C\bar{\nu}B$  capture rate may have a slight distortion only when  $\theta_{13}$  is sufficiently large, as shown in Fig. 4(e) and Fig. 4(f). Hence it is in practice almost impossible to probe the magnitude of  $\theta_{13}$  by detecting the  $C\bar{\nu}B$ .

(3) The  $Q$ -value may sensitively affect the absolute capture rate of relic antineutrinos, but it does not influence the relative locations of the signature and its corresponding background. This property is illustrated in Fig. 5, where the smallest neutrino mass (i.e.,  $m_1$  in the  $\Delta m_{31}^2 > 0$  case or  $m_3$  in the  $\Delta m_{31}^2 < 0$  case) has been taken to be zero for simplicity. Allowing  $Q$  to vary from 2.3 keV to 2.8 keV, we find that the absolute capture rate undergoes a decrease of as much as one order of magnitude. The reason for this feature can be explained with the help of Eq. (8). The binding energies  $E_i$  of the seven available atomic levels are all smaller than 2.1 keV, and thus the individual capture rates at  $T_k \equiv E_{\bar{\nu}_k} + Q$  are strongly suppressed by the corresponding Breit-Wigner distributions.

A larger  $Q$ -value implies a stronger suppression of the overall capture rate  $\lambda_{\bar{\nu}}$ , leading to a worse signature of the  $C\bar{\nu}B$  in the experiment. That is why the isotope of a smaller  $Q$ -value is eagerly wanted [13], in order to make this interesting  $C\bar{\nu}B$  detection method more feasible in the foreseeable future.

In summary, we have examined the flavor effects on a possible detection of the  $C\bar{\nu}B$  by using a target made of  $^{163}\text{Ho}$  nuclei. On the one hand, we have discussed the energy spectrum of the EC decay of  $^{163}\text{Ho}$  by looking at how sensitive the ratios of the peak heights and the fine structure near the spectral endpoint are to the neutrino mass hierarchy. On the other hand, we have presented a detailed analysis of the effects of different neutrino masses and reasonable values of the smallest neutrino mixing angle  $\theta_{13}$  on the relic antineutrino capture rate and the corresponding EC decay background. Our results demonstrate that such flavor effects, which were not considered in Ref. [13], can be appreciable and even important in some cases.

At least three factors may apparently affect the observability of relic antineutrinos in such a calorimetric experiment. The first one is the number of the target particles  $N_T$ , which is the only adjustable parameter for a given measurement to increase the total capture events. In our numerical analysis we have taken 30 kg  $^{163}\text{Ho}$  as a reference isotope source, just for the purpose of illustration. The second factor is the finite energy resolution  $\Delta$ , which has a crucial impact on the signature-to-background ratio. As the precision of  $\Delta$  is gradually improved, it should be possible to establish a signature of relic antineutrinos just beyond the spectral endpoint of the EC decay of  $^{163}\text{Ho}$  in the future. If the energy resolution were really perfect, we would even be able to resolve the multiple peaks coming from different neutrino mass eigenstates and then obtain some information on neutrino masses and flavor mixing angles. But it will be a great success even if only a single peak of the signature can in practice be resolved. The third factor is the number density of relic antineutrinos  $n_{\bar{\nu}_k}$  (for  $k = 1, 2, 3$ ) around the Earth. Its value might be much larger than  $n_{\nu_k} = n_{\bar{\nu}_k} \simeq 56 \text{ cm}^{-3}$  predicted by the standard Big Bang cosmology, if the gravitational clustering effect is significant [19]. A larger value of  $n_{\bar{\nu}_k}$  will always be a good news for the detection of the  $C\bar{\nu}B$ .

To conclude, the  $C\nu B$  and  $C\bar{\nu}B$  can in principle be detected by means of the  $\beta$ -decaying nuclei (e.g.,  $^3\text{H}$ ) and the EC-decaying nuclei (e.g.,  $^{163}\text{Ho}$ ), respectively. Although the present experimental techniques are unable to lead us to a guaranteed measurement of relic neutrinos and antineutrinos in the near future, we might be able to make a success of this great exploration in the long term. At least from a historical point of view, nothing is completely hopeless in neutrino physics.

This work was supported in part by the China Postdoctoral Science Foundation under grant No. 20100480025 (Y.F.L.) and in part by the National Natural Science Foundation of China under grant No. 10875131 (Z.Z.X.).

## References

- [1] See, e.g., Z.Z. Xing and S. Zhou, *Neutrinos in Particle Physics, Astronomy and Cosmology* (Zhejiang University Press and Springer-Verlag, 2011).
- [2] For a brief review, see: A. Ringwald, Nucl. Phys. A **827**, 501c (2009).
- [3] S. Weinberg, Phys. Rev. **128**, 1457 (1962).
- [4] J.M. Irvine and R. Humphreys, J. Phys. G **9**, 847 (1983).
- [5] A. Cocco, G. Mangano, and M. Messina, JCAP **0706**, 015 (2007).
- [6] R. Lazauskas, P. Vogel, and C. Volpe, J. Phys. G **35**, 025001 (2008).
- [7] M. Blennow, Phys. Rev. D **77**, 113014 (2008).
- [8] R. Hodak, S. Kovalenko, and F. Simkovic, AIP Conf. Proc. **1180**, 50 (2009).
- [9] Y.F. Li, Z.Z. Xing, and S. Luo, Phys. Lett. B **692**, 261 (2010); Y.F. Li and Z.Z. Xing, Phys. Lett. B **695**, 205 (2011).
- [10] A. Kabout, J.A. Formaggio, and B. Montreal, Phys. Rev. D **82**, 062001 (2010).
- [11] A. Faessler *et al.*, arXiv:1102.1799.
- [12] A.G. Cocco, G. Mangano, and M. Messina, Phys. Rev. D **79**, 053009 (2009).
- [13] M. Lusignoli and M. Vignati, Phys. Lett. B **697**, 11 (2011).
- [14] See, e.g., F. Gatti *et al.*, Phys. Lett. B **398**, 415 (1997); F. Gatti *et al.*, J. Low Temp. Phys. **151**, 603 (2008); A. Nucciotti (MARE Collaboration), arXiv:1012.2290.
- [15] Particle Data Group, K. Nakamura *et al.*, J. Phys. G **37**, 075021 (2010).
- [16] M.C. Gonzalez-Garcia, M. Maltoni, and J. Salvado, JHEP **1004**, 056 (2010).
- [17] W. Bambus, Rev. Mod. Phys. **49**, 77 (1977) [Erratum-ibid. **49**, 961 (1977)].
- [18] A. De Rujula and M. Lusignoli, Phys. Lett. B **118**, 429 (1982).
- [19] A. Ringwald and Y.Y.Y. Wong, JCAP **0412**, 005 (2004).
- [20] E. Komatsu *et al.* (WMAP Collaboration), Astrophys. J. Supp. **192**, 18 (2011).

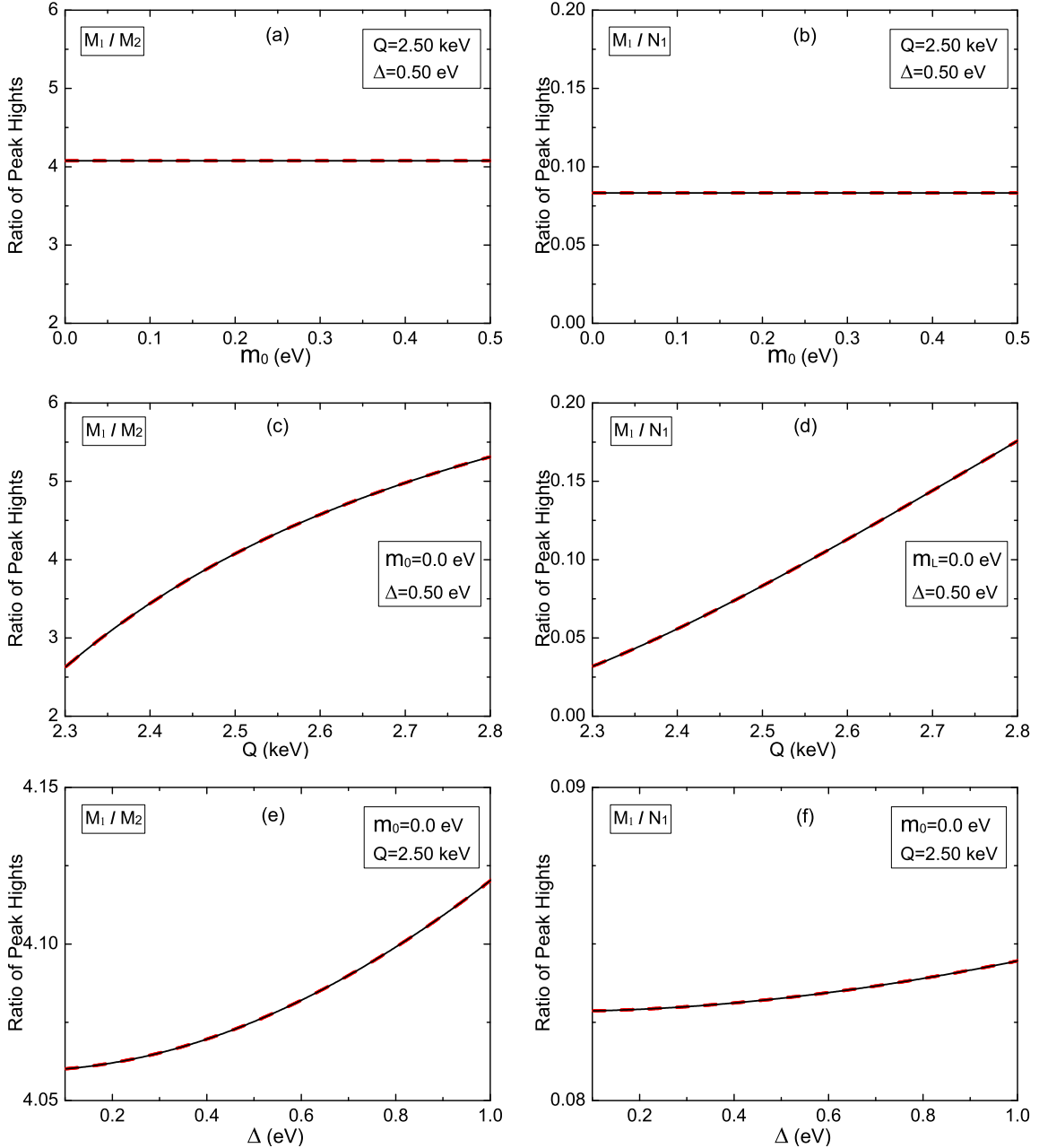


Figure 1: The energy spectrum of the EC decay of  $^{163}\text{Ho}$ : the ratios of the peak heights  $M_1/M_2$  and  $M_1/N_1$  changing with the lightest neutrino mass  $m_0$  (equal to  $m_1$  in the  $m_{31}^2 > 0$  case with a solid curve or to  $m_3$  in the  $m_{31}^2 < 0$  case with a dashed curve), the  $Q$ -value and the energy resolution  $\Delta$ . Here  $\theta_{13} = 10^\circ$  has typically been input.

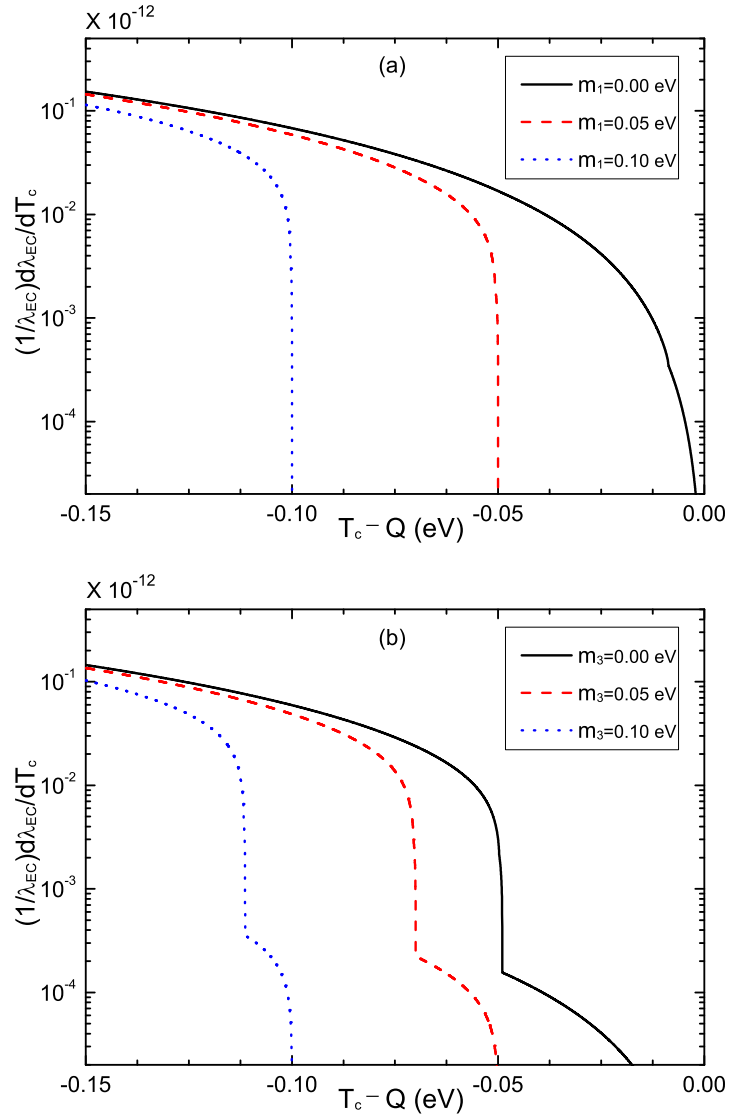


Figure 2: The energy spectrum of the EC decay of  $^{163}\text{Ho}$ : the fine structure near its endpoint in the  $m_{31}^2 > 0$  (top panel) or  $m_{31}^2 < 0$  (bottom panel) case. Here  $Q = 2.5$  keV and  $\theta_{13} = 10^\circ$  have typically been input.

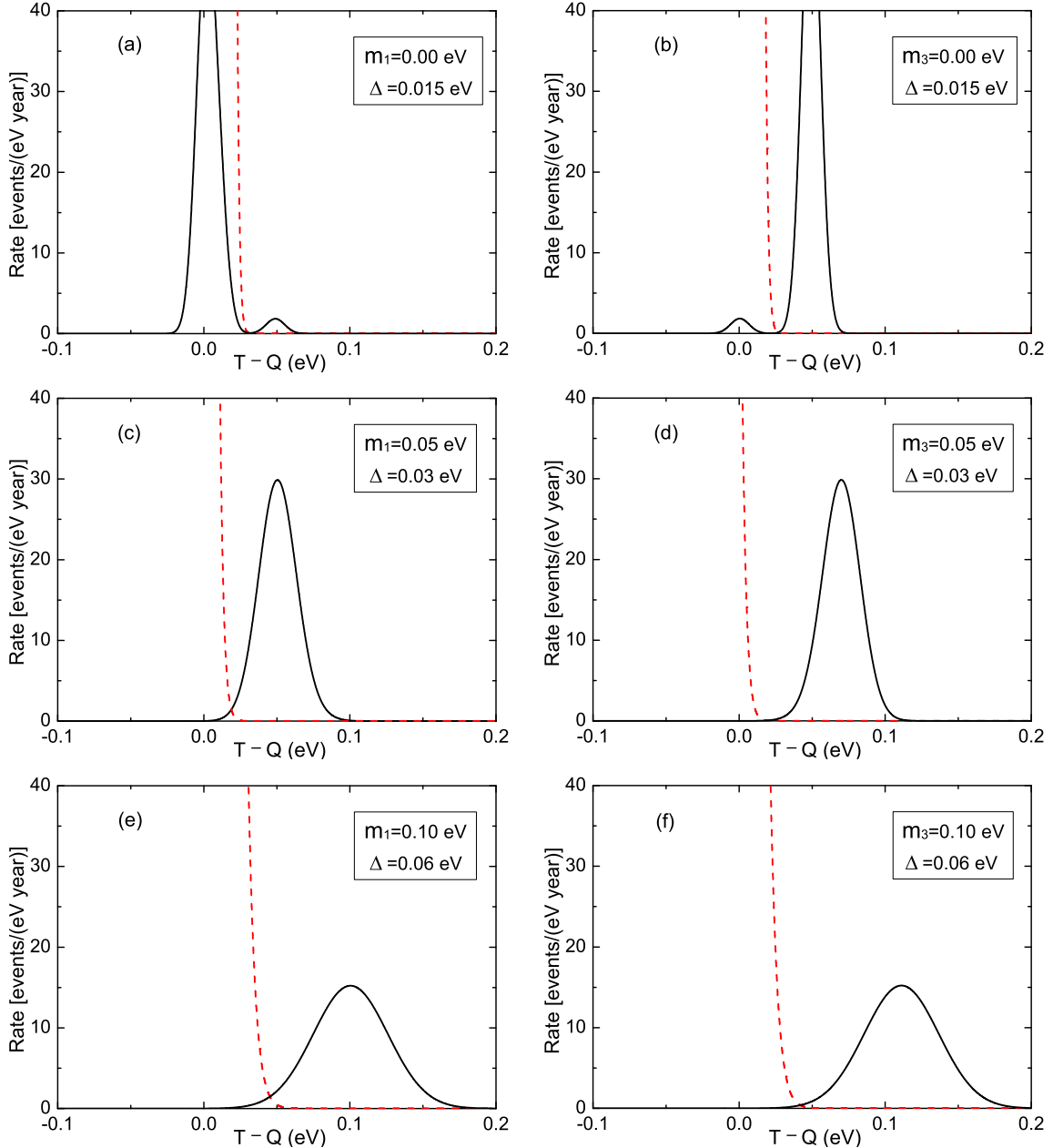


Figure 3: The relic antineutrino capture rate as a function of the overall energy release  $T$  in the  $\Delta m_{31}^2 > 0$  (left panel) or  $\Delta m_{31}^2 < 0$  (right panel) case. The solid and dashed curves represent the  $C\bar{\nu}B$  signature and its background, respectively. The value of the finite energy resolution  $\Delta$  is chosen in such a way that only a single peak of the signature can be seen. Here  $\theta_{13} = 10^\circ$  has typically been input.

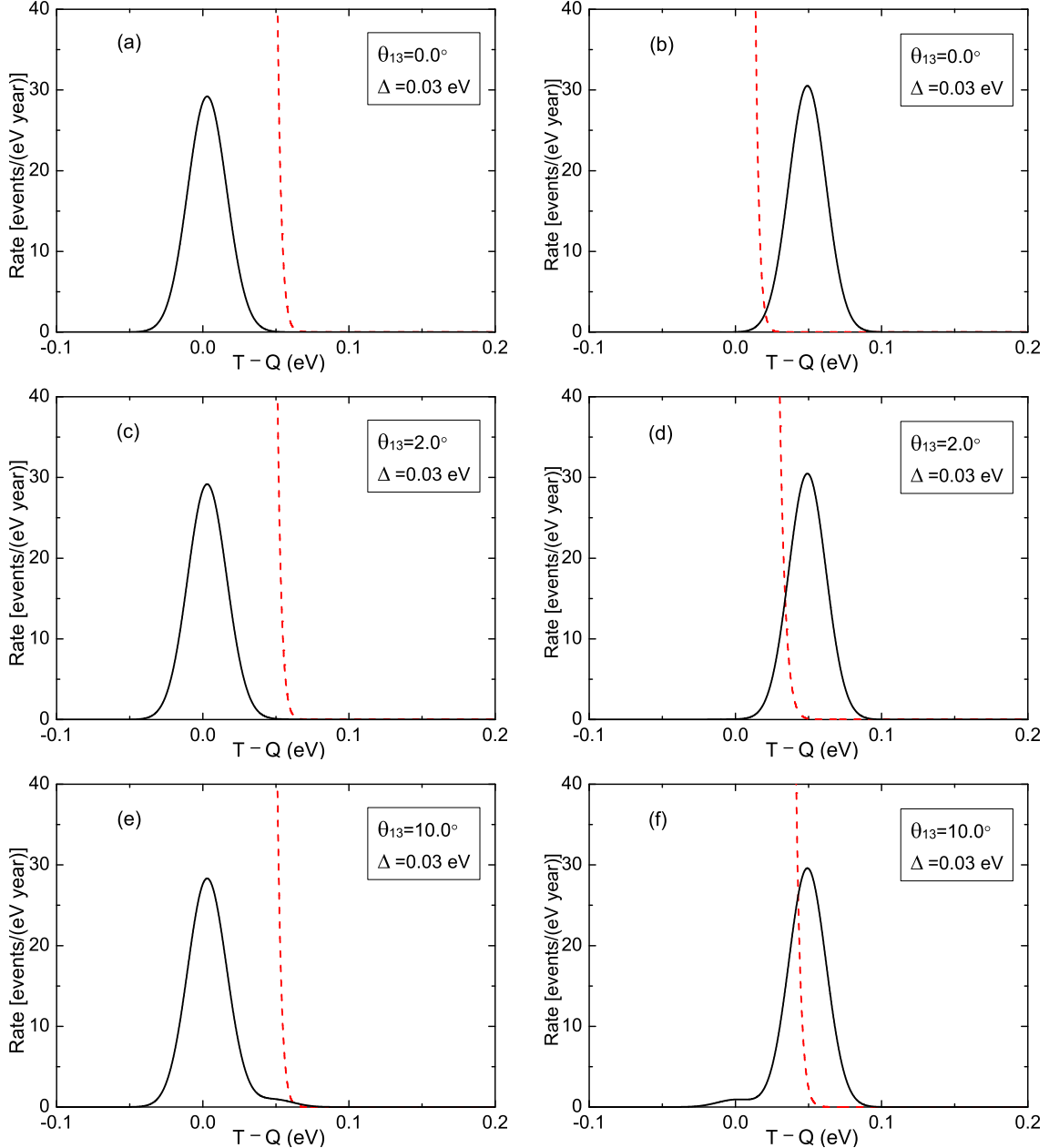


Figure 4: The relic antineutrino capture rate as a function of the overall energy release  $T$  in the  $\Delta m_{31}^2 > 0$  case with  $m_1 = 0$  (left panel) or in the  $\Delta m_{31}^2 < 0$  case with  $m_3 = 0$  (right panel). The solid and dashed curves represent the  $C\bar{\nu}B$  signature and its background, respectively. The value of the finite energy resolution  $\Delta$  is chosen in such a way that the signature in Fig. 4(b) with  $\theta_{13} = 0^\circ$  should be clearly seen.

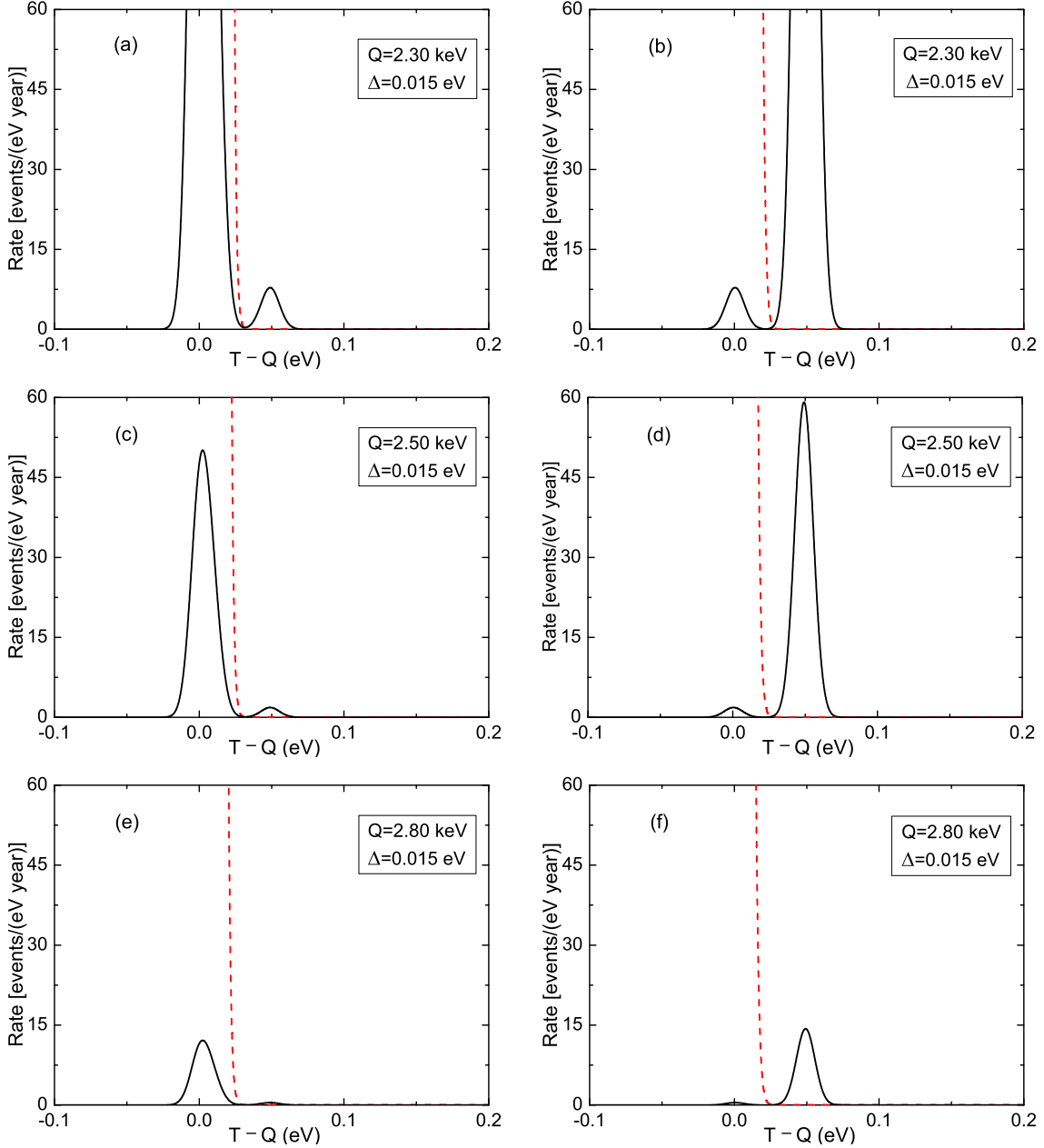


Figure 5: The relic antineutrino capture rate as a function of the overall energy release  $T$  in the  $\Delta m_{31}^2 > 0$  case with  $m_1 = 0$  (left panel) or in the  $\Delta m_{31}^2 < 0$  case with  $m_3 = 0$  (right panel). The solid and dashed curves represent the  $\text{C}\bar{\nu}\text{B}$  signature and its background, respectively. The value of the finite energy resolution  $\Delta$  is chosen in such a way that only a single peak of the signature can be seen. Here  $Q = 2.3$  keV, 2.5 keV and 2.8 keV together with  $\theta_{13} = 10^\circ$  have typically been input.